

# Design and Assessment of Lead–sCO<sub>2</sub> Intermediate Heat Exchanger for LFRs

Fanli Kong<sup>1,2</sup>, Chi Xu<sup>1,2</sup>, Yijiang Fan<sup>1,2</sup>, Dali Yu<sup>1,3,\*</sup>, Jie Yu<sup>1</sup>, Shuyong Liu<sup>1</sup>

<sup>1</sup>Institute of Nuclear Energy Safety Technology, HFIPS, Chinese Academy of Sciences, Hefei 230031, China

<sup>2</sup>University of Science and Technology of China, Hefei 230026, China

<sup>3</sup>Key Laboratory of Advanced Reactor Engineering and Safety, Ministry of Education, Tsinghua University, Beijing 100084, China

**Abstract.** Lead–sCO<sub>2</sub> intermediate heat exchanger (IHX) was designed for lead-cooled fast reactor (LFR). The reactor coolant is lead and flowing through a circular straight channel, meanwhile, sCO<sub>2</sub> is heated through 5 channels with different geometries were investigated respectively, including straight channel, zigzag 52° channel, S-shaped fins, offset rectangular fins, and airfoil fins. Considering the thermal-hydraulics characteristics, mechanical structure, corrosion, and flow blockage in the IHX designs, the performance, total cost, and power density of several heat exchanger designs were evaluated and compared. Finally, a printed circuit heat exchanger (PCHE) design using the circular straight (lead) - offset rectangular fins (sCO<sub>2</sub>) channels was proposed. The straight and S-shaped channels for sCO<sub>2</sub> flow were recommended as alternative designs under certain circumstances. However, S-shaped fins and zigzag channels will dramatically increase the cost while straight and airfoil channels will greatly increase the volume.

## 1 Introduction

As a Generation IV nuclear reactor system, the lead-cooled fast reactors (LFRs) have the advantages of high safety, good economy, and compact structure<sup>[1]</sup>. LFRs coupling with the supercritical carbon dioxide (sCO<sub>2</sub>) power cycle is a promising solution for the miniaturization and modularization of nuclear power systems<sup>[2]</sup>. The intermediate heat exchanger (IHX) should work normally under the conditions with high temperature, high pressure, and high pressure difference of the heat transfer fluid on both sides (nearly normal pressure on the lead side and high pressure over 20 MPa on the sCO<sub>2</sub> side).

The printed circuit heat exchanger (PCHE) is particularly suitable to be applied as an IHX due to the advantages of large heat exchange area per unit volume, high overall heat transfer coefficient, high temperature resistance, and high pressure resistance<sup>[3]</sup>. Currently, there are mainly two types of flow channels for PCHE developed and classified in terms of surface geometries: the continuous types including the straight and zigzag channels, and the discontinuous channels including S-shaped, airfoil, and offset rectangular fins<sup>[4]</sup>. Based on the application of the straight channel, the zigzag channel design has been developed to enhance the heat transfer performance, however, this design increases the pressure drop accordingly<sup>[5]</sup>. Researchers developed and investigated the S-shaped fins, airfoil fins, and discontinuous offset rectangular fins to reduce the pressure drop<sup>[6-8]</sup>.

With the increasing research on the sCO<sub>2</sub> cycle, studies on PCHEs for advanced reactors have been developed including tasks on thermal-hydraulic performance, stress analysis, cost assessment, and optimization of geometrical parameters<sup>[3, 9-10]</sup>. Yoon et al.<sup>[11]</sup> studied different PCHE types of IHXs of both High Temperature Gas-cooled Reactors (HTGRs) and Sodium-cooled Fast Reactors (SFRs) and concluded that it is recommended to use zigzag PCHE for IHXs in HTGRs, and use straight PCHE for SFRs in consideration of both thermal-hydraulic performance and cost. Kim et al.<sup>[12]</sup> evaluated different flow channel PCHEs for FLiNaK to sCO<sub>2</sub> heat exchanger in Fluoride salt-cooled High-temperature Reactors (FHRs) and proposed several recommended channel configurations, but no conclusion has been given on which type of channel is more recommended and there are few studies considering thermal-hydraulic performance, mechanical design, and cost assessment of IHXs in LFRs.

In this study, we developed a promising design for a lead–sCO<sub>2</sub> IHX in LFRs. The thermal-hydraulics, mechanical design, corrosion and blockage issues were considered in the design. The different types of flow channels including the straight channel, zigzag 52° channel, S-shaped fins, offset rectangular fins and airfoil fins were investigated. The thermal and hydraulic performance, total cost and power density of different type IHXs were evaluated to select the highest performance design.

\* Corresponding author: [dlyu@inest.cas.cn](mailto:dlyu@inest.cas.cn)

## 2 Considerations for IHX design

### 2.1 Reference conditions

Parameters of a reference nuclear reactor, STAR-LM, and the sCO<sub>2</sub> recompression Brayton power generation system<sup>[13]</sup> were selected as operating conditions of IHX which are modified to a larger log mean temperature difference, shown in Table 1. The properties of the liquid lead and sCO<sub>2</sub> were obtained through the NEA handbook<sup>[14]</sup> and the NIST chemistry web-book<sup>[15]</sup>, respectively.

**Table 1.** Operating conditions for IHX

IHX	$T_{in} / ^\circ C$	$T_{out} / ^\circ C$	$p / MPa$	Mass flow rate / kg·s <sup>-1</sup>
Lead	578	438	0.1	19708
sCO <sub>2</sub>	402.5	550	20	2205

### 2.2 Surface geometry selection and structural design

For the lead side, the straight circular channel was selected on the lead side. For the circular channel on the lead side, the double banking setup is used, and the structure is shown in Figure 1. For the sCO<sub>2</sub> side, several types of surface geometry mentioned above are selected. (Figure 2). IHX is composed of module groups with a maximum module size of 600 mm × 3000 mm × 1500 mm (W × H × L).

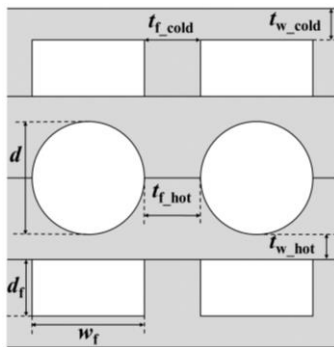


**Figure 1.** The cross-sectional view of the configuration

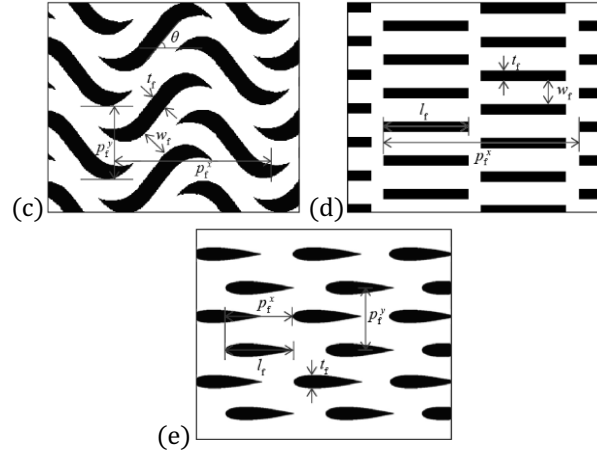
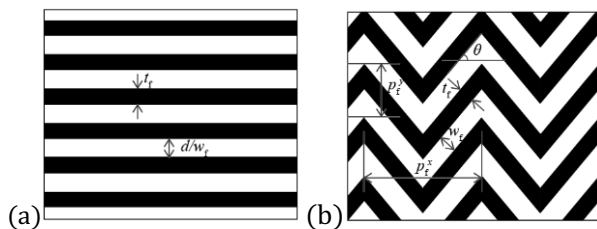


**Figure 2.** Schematic of channel (a. Straight channel b. Zigzag 52° channel c. S-shaped channel d. Offset rectangular fins e. NACA0020 airfoil fins)

### 2.3 Thermal-hydraulic Correlations

The Seban-Shimazaki correlation was used to calculate the Nusselt number of liquid, shown as Eq. (1)<sup>[16]</sup>. The friction factor correlation for other fluids can be applied to the liquid metal. Table 2 shows the thermal-hydraulic correlations available for PCHEs which can be applied to the sCO<sub>2</sub> flow.

$$Nu = 5.0 + 0.025(RePr)^{0.8} \quad (1)$$

**Table 2.** Thermal-hydraulic correlations for PCHEs

Types of channel	Cross section	Correlations
Straight channel	semi-circle or circle $d = 2.10$ mm $D_e = 2.10 / 1.28$ mm (circle/semi-circle)	Laminar $f = 15.78/Re$ $Nu = 4.089$
		Turbulent $f = (0.790 \ln Re - 1.64)^{-2}$ $Nu = \frac{(f/8)(Re - 1000)Pr}{1 + 12.7(f/8)^{1/2}(Pr^{2/3} - 1)}$ $3000 < Re < 5 \times 10^6$ $0.5 < Pr < 2000$ [13]
Zigzag 52° channel	Rectangular $\theta = 52^\circ$ $w_f = 1.51$ mm $d_f = 1.09$ mm $D_e = 1.26$ mm	Turbulent $f = 0.1924Re^{-0.091}$ $Nu = 0.1696Re^{0.629} Pr^{0.317}$ $3.5 \times 10^3 < Re < 2.2 \times 10^4$ $0.75 < Pr < 2.2$ [13]
S-shaped fin	Rectangular $\theta = 52^\circ$ $w_f = 1.31$ mm $d_f = 0.94$ mm $D_e = 1.09$ mm	Turbulent $f = 0.4545Re^{-0.340}$ $Nu = 0.1740Re^{0.593} Pr^{0.430}$ $3.5 \times 10^3 < Re < 2.3 \times 10^4$ $0.75 < Pr < 2.2$ [13]
Offset rectangular fin	Rectangular $w_f = 1.95$ mm	Turbulent $f = 0.0276$ $Nu = 0.1034Re^{0.7054} Pr^{0.3489}$

	$d_t = 0.65$ mm $k = 7.69$ mm $D_e = 0.95$ mm	$2700 < Re < 3.8 \times 10^4$ $0.8 < Pr < 25$ [4]
NACA0020 airfoil fin	$k = 4$ mm $d_t = 0.95$ mm $D_e = 1.205$ mm	Turbulent $f = 0.0256$ $Nu = 0.0601Re^{0.7326}Pr^{0.3453}$ $2700 < Re < 3.8 \times 10^4$ $0.8 < Pr < 25$ [4]

### 3 Modelling of IHX design

#### 3.1. Thermal design model

The total heat transfer coefficient is defined by the hot side and the required heat transfer area can be calculated through Eq. (2)-(4). According to the actual total heat transfer area, the required length of the heat exchanger is obtained.

$$\frac{1}{U} = \frac{1}{h_{hot}} + \frac{A_{s,hot} \Delta t_w}{A_{s,w} \lambda_w} + \frac{A_{s,hot}}{A_{s,cold} h_{cold}} \quad (2)$$

$$A_{s,r} = \frac{Q}{U \Delta T_{lm}} \quad (3)$$

$$L_r = \frac{L A_{s,r}}{A_{s,a}} \quad (4)$$

#### 3.2 Structural model

In this work, the determination of edge thickness ( $t_e$ ), fin thickness ( $t_f$ ), and wall thickness ( $t_w$ ) were considered in the preliminary structural design. The conservative model design method<sup>[17]</sup> was adopted to carry out the preliminary mechanical design.

Taking the fin thickness and the wall thickness as an example, the design criteria can be expressed as Eq. (5)-(7):

$$S_m^S \leq SE \quad (5)$$

$$S_m^L \leq SE \quad (6)$$

$$S_t^L = S_m^L + S_b^L \leq 1.5SE \quad (7)$$

where S is the maximum allowable stress and E is the joint factor.

And the stress values mentioned above can be expressed as Eq. (8)-(10):

$$S_m^S = \frac{ph}{t_f} \quad (8)$$

$$S_m^L = \frac{pH}{2t_w} \quad (9)$$

$$S_b^L = \frac{ph^2c}{12I} \quad (10)$$

where  $p$ ,  $h$ ,  $H$  are the design pressure, the channel width and the channel depth, respectively.

The distance from neutral axis to extreme  $c$  and the moment of inertia  $I$  can be computed by Eq. (11):

$$I = \frac{t_w^3}{12}, \quad c = \frac{t_w}{2} \quad (11)$$

Similarly, the edge thickness can be designed by using the same design criteria.

#### 3.3 Economic model

To compare and optimize the design of IHXs, an economic evaluation model was introduced to quantify the performance of each design.

Firstly, the total investment cost ( $C_i$ ) is simplified to include only capital cost ( $C_{cp}$ ) and operating cost ( $C_o$ ) without considering the costs of manufacturing, heads, labor and others, as shown in Eq. (12)<sup>[18]</sup>:

$$C_i = C_{cp} + C_o \quad (12)$$

The capital cost is calculated by Eq. (13) and (14):

$$C_c = C_M M = C_M \rho_M V \quad (13)$$

$$C_{cp} = \frac{C_c r(1+r)^n}{[(1+r)^n - 1]} \quad (14)$$

where  $C_M$  is price of materials per kilogram,  $n$  is the payback year set to 20 and  $r$  is the interest rate set to 4%. The operating cost was analyzed by calculating the pump work and the cost of electricity cost:

$$C_o = C_E \frac{\Delta p \dot{m}}{\rho} \quad (15)$$

where  $C_E$  is the average price of electricity for the industrial sector which is set to 0.0000947 \$·W<sup>-1</sup>·h<sup>-1</sup><sup>[19]</sup>.

## 4 Analysis and Results

#### 4.1 Heat transfer coefficient

Since the circular straight channel on the lead side was selected and fixed when changing the surface type on the sCO<sub>2</sub> side, the surface type on the sCO<sub>2</sub> side was used to denote the IHX type.

As shown in Figure 3, the overall heat transfer coefficients of the zigzag, offset rectangular, and S-shaped IHXs are about two times higher than the heat transfer coefficients of straight and airfoil IHXs for specific design.

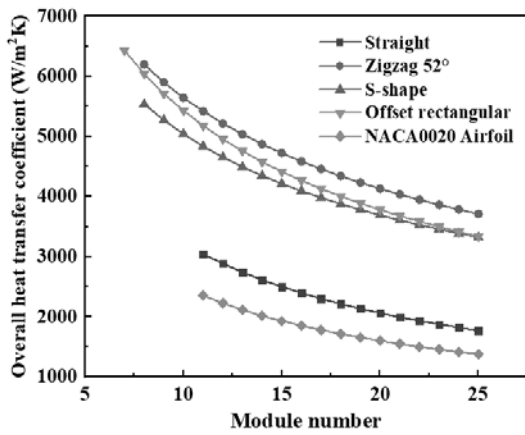


Figure 3. Overall heat transfer coefficient vs. module number

### 4.2 Pressure drop

Figure 4 and 5 show that the pressure drop on both sides of the offset rectangular IHX is the lowest. In the design calculation, the pressure drop on the lead side is set to be less than 50 kPa. The pressure drop of zigzag IHX on the cold side is much larger than the other types. The offset rectangular, S-shaped, and zigzag IHXs can meet the pressure drop requirement on the lead side with a smaller module number.

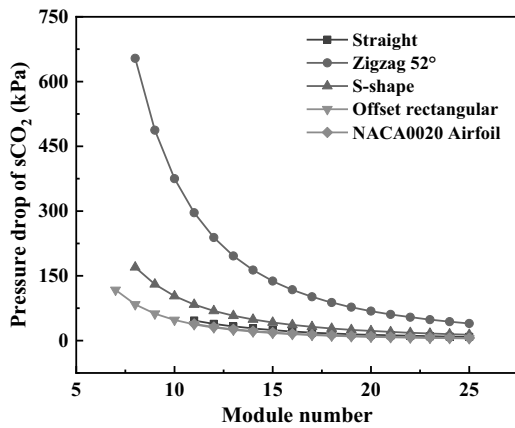


Figure 4. Pressure drop (sCO<sub>2</sub>) vs. module number

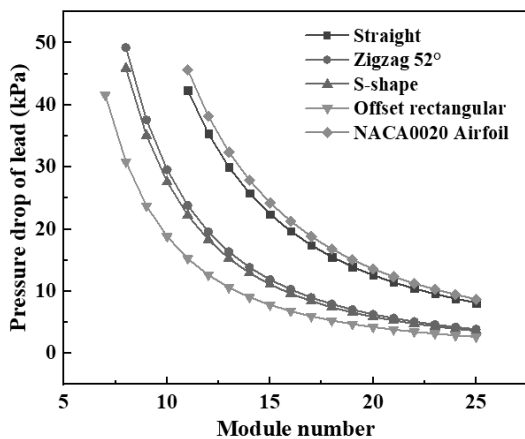


Figure 5. Pressure drop (Lead) vs. module number

### 4.3 Cost analysis

To evaluate the design of IHX, the cost of IHX for different surface type configurations is varying with the module number shown in Figure 6. The cost of IHX with the offset rectangular fins on the sCO<sub>2</sub> side was the lowest, while that of the zigzag channel was the highest. The others are airfoil fins, straight channel, and S-shaped fins from low to high. However, the cost of the S-shaped fins can be lower than the cost of the airfoil fins and straight channels when the module number increases.

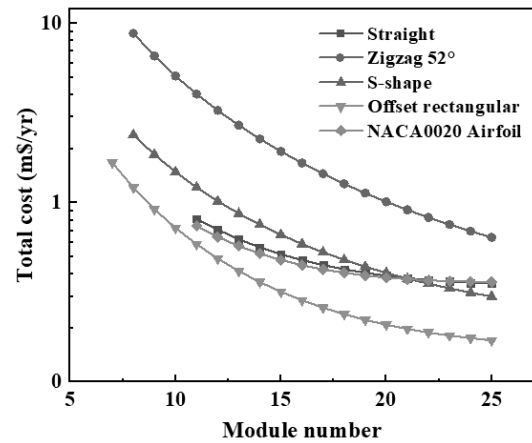


Figure 6. Total cost vs. module number

### 4.4 Power density

As a key component coupled with a compact sCO<sub>2</sub> power cycle, the power density of IHX is also critical. The power density (the heat rate per volume) of different types of IHXs is shown in Figure 7. The offset rectangular fins have the highest power density, followed by the zigzag channel, S-shaped fins, straight channel, and airfoil fins in the order from high power density to low power density. Among all the lower-cost IHX types, including the straight channel, S-shaped fins, and airfoil fins, only the S-shaped fins provide relatively good power density and the others don't. Though the zigzag channel has the largest cost, it ranks second in power density.

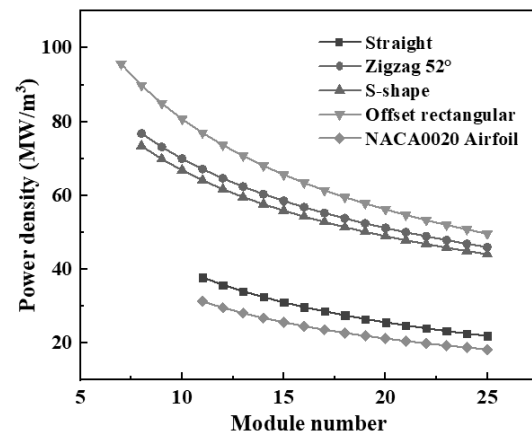


Figure 7. Power density vs. module number

## 5 Conclusions

PCHEs with different surface geometry types were designed and the performance, total cost, and power density were evaluated. The conclusions have been drawn as follows:

- (1) For the lead side, the circular straight channel was used since it can reduce the corrosion and flow blockage effect. Besides, it is not a priority to enhance heat transfer by optimizing the surface geometry on the lead side because the heat transfer coefficient on the lead side is about 10-20 times larger than that on the sCO<sub>2</sub> side.
- (2) The circular straight (lead) - offset rectangular fins (sCO<sub>2</sub>) PCHE is the recommended design for IHX in the LFRs. It has the lowest total cost, high power density, and excellent thermal-hydraulic performance. The straight and S-shaped channels for sCO<sub>2</sub> would be alternative designs under certain circumstances which the size or cost restrictions are not very strict.

This study preliminarily proposed a PCHE type IHX design, which provides a solution to lead-sCO<sub>2</sub> IHX design in a nuclear power system of LFR coupling with sCO<sub>2</sub> power cycle. Furthermore, the optimization of IHX considering the impacts of hydraulic diameter, heat exchanger effectiveness, and the effects on the power cycle efficiency, would be implemented in future work.

## Acknowledgement

This work was supported by the Ministry of Education Key Laboratory of Advanced Reactor Engineering and Safety Project, Grant No. ARES-2020-04 and Key Supporting Program of 13<sup>th</sup> five-year plan, CASHIPS (KP-2019-11).

## References

1. A. Alemberti, V. Smirnov, C. F. Smith, et al. *Prog. Nucl. Energ.* **77**: 300–307 (2014).
2. F. Kong, Y. Li, R. Sa, et al. *Int. J. Energ. Res.* **43**(9): 4940–4948 (2019).
3. M. Chen. Ann Arbor, MI, USA: University of Michigan (2018).
4. S. R. Pidaparti, M. H. Anderson, D. Ranjan. *Exp. Therm. Fluid Sci.* **106**: 119–129 (2019).
5. D. E. Kim, M. H. Kim, J. E. Cha, et al. *Proceedings of KSME conference* (2008).
6. N. Tsuzuki, Y. Kato, T. Ishiduka. *Appl. Therm. Eng.* **27**(10): 1702–1707 (2007).
7. D. E. Kim, M. H. Kim, J. E. Cha, S. O. Kim. *Nucl. Eng. Des.* **238**(12): 3269–3276 (2008).
8. X. Xu, Q. Wang, L. Li, S. V. Ekkad, T. Ma. *Numer. Heat Tr. A-Appl.* **68**(10): 1067–1086 (2015).
9. L. Chai, S. A. Tassou. *Therm. Sci. Eng. Prog.* **18** (2020).
10. Zhang X. Columbus, OH, USA: The Ohio State University (2015).
11. S. H. Yoon, H. C. No, G. B. Kang. *Nucl. Eng. Des.* **270**: 334–343 (2014).
12. I. H. Kim, X. Zhang, R. Christensen, X. Sun. *Ann. Nucl. Energy.* **94**: 129–137 (2016).
13. A. Moisseytsev, J. J. Sienicki. *Nucl. Eng. Des.* **238**(8): 2094–2105 (2008).
14. C. Fazio C, V. P. Sobolev, A. Aerts, et al. *NEA of the OECD: NEA—7268* (2015).
15. U.S. Department of Commerce. *NIST chemistry web-book [EB/OL]*. <https://webbook.nist.gov/chemistry/fluid/>.
16. S. M. Kissick, H. Wang. *the ASME 2018 IMECE* (2018).
17. R. Pierres, D. Southall, S. Osborne. *Proceedings of sCO<sub>2</sub> Power Cycle Symposium* (2011).
18. I. H. Kim, H. C. No. *Nucl. Eng. Des.* **243**: 243–250 (2012).
19. Y. Hu. *Price: Theory and Practice.* **07**: 69–72 (2019) (in Chinese).